Release of VEGF and BMP9 from injectable alginate based composite hydrogel for treatment of myocardial infarction

Yong Wu[a], Tianqi Chang[a], Weiqian Chen[a], Xiaoyu Wang[a], Jingjing Li[a], Yueqiu Chen[a], You Yu[a], Zhenya Shen[a,***], Qian Yu[b,**], Yanxia Zhang[a,*]

[a] Institute for Cardiovascular Science & Department of Cardiovascular Surgery of the First Affiliated Hospital, Medical College, Soochow University, Suzhou, 215000, PR China
[b] State and Local Joint Engineering Laboratory for Novel Functional Polymeric Materials, College of Chemistry, Chemical Engineering and Materials Science, Soochow University, Suzhou, 215123, PR China

ARTICLE INFO

ABSTRACT

Myocardial infarction (MI) is one of cardiovascular diseases that pose a serious threat to human health. The pathophysiology of MI is complex and contains several sequential phases including blockage of a coronary artery, necrosis of myocardial cells, inflammation, and myocardial fibrosis. Aiming at the treatment of different stages of MI, in this work, an injectable alginate based composite hydrogel is developed to load vascular endothelial active factor (VEGF) and silk fibroin (SF) microspheres containing bone morphogenetic protein 9 (BMP9) for releasing VEGF and BMP9 to realize their respective functions. The results of in vitro experiments indicate a rapid initial release of VEGF during the first few days and a relatively slow and sustained release of BMP9 for days, facilitating the formation of blood vessels in the early stage and inhibiting myocardial fibrosis in the long-term stage, respectively. Intramyocardial injection of such composite hydrogel into the infarct border zone of mice MI model via multiple points promotes angiogenesis and reduces the infarction size. Taken together, these results indicate that the dual-release of VEGF and BMP9 from the composite hydrogel results in a collaborative effect on the treatment of MI and improvement of heart function, showing a promising potential for cardiac clinical application.

1. Introduction

Cardiovascular disease is a serious threat to human health, which accounted for the first cause of death among Americans in 2017 according to the latest data of the American Heart Association (AHA) in 2020 [1]. The 2019 American College of Cardiology (ACC)/AHA Guidelines for Primary Prevention of Cardiovascular Diseases indicated that atherosclerotic cardiovascular disease remained the main cause of global morbidity and mortality [2]. One of the common cardiovascular diseases is myocardial infarction (MI) due to local ischemia and hypoxia caused by coronary artery occlusion, which in turn causes myocardial cell damage and necrosis. The progress of MI process usually leads to late myocardial fibrosis, and even weakened ventricular contraction and diastolic function, eventually inducing malignant arrhythmia, heart failure (HF) or sudden death [3,4]. Currently, the main

clinical treatments for MI include thrombolysis with medicine, percutaneous coronary intervention and coronary artery bypass grafting [5–7]. Although these methods can certainly alleviate MI symptoms, they are difficult to repair and reconstruct the damaged or infarcted myocardium. Stem cell-based therapies for cardiac repair hold great promise [8], however, the retention and survival rate of the injected stem cells are relatively low due to the harsh microenvironment (e.g. ischemia, hypoxia, inflammation) in the MI area, resulting in poor long-term effectiveness [9]. It is indicated that in the improvement of cardiac function the stem cells act through paracrine mechanisms by secreting some bioactive factors (e.g., vascular endothelial active factor (VEGF), platelet derived growth factor (PDGF), stromal cell derived factor-1 (SDF-1)) [10–13]. Therefore, it is suggested to be an effective way to treat MI by introducing appropriate bioactive factors to promote the corresponding physiological behaviors conforming the

pathophysiological process of MI.

Previous studies have shown that in the early stage of MI, application of angiogenesis-related active factors, such as VEGF could promote the proliferation and migration of endothelial cells and formation of new blood vessels in the infarct area ultimately. The newly formed vessels not only improve the harsh MI microenvironment to prevent the further expansion of the infarction area, but also benefit the establishment of collateral circulation to enhance blood supply, preventing further necrosis of cardiomyocytes in the infarct border area and improving the therapeutic effect of VEGF [14,15]. Moreover, in the middle and late stage of MI, introduction of bioactive factors to inhibit myocardial fibrosis (the transformation from myocardial fibroblasts to myofibroblasts) has been recognized as a promising way to prevent HF [16–18]. The latest researches showed that in the HF mice model, the process of myocardial fibrosis was slowed down effectively via the treatment of bone morphogenetic protein 9 (BMP9) [19,20], which is an endogenous inhibitor of myocardial fibrosis by inhibiting the effect of transforming growth factor β1 (TGF-β1). However, because of the uncontrolled release of VEGF or BMP9, high doses of such bioactive factors must be used to compensate for the short half-life, high diffusion rate and low activity under hypoxic-ischemic conditions to realize their clinical effects. Therefore, it is required a proper carrier system that can release VEGF and BMP9 in different manners to conform the different stages of MI for the better treatment.

In recent years, injectable hydrogels based on natural polymers (e.g. alginate, fibrin, collagen and self-assembled peptides) have been used as carriers for loading and releasing of bioactive factors to treat MI [21–28]. For example, alginate, a type of anionic natural polysaccharide, can be crosslinked with divalent cations under mild physiological conditions to form hydrogel with a certain viscosity and mechanical strength [29]. In addition, the alginate hydrogel has good biocompatibility and mechanical properties similar to the extracellular matrix (ECM), and thus can provide temporary structural support for damaged myocardium when it is applied to the infarct site to limit ventricular expansion [30–34]. In addition, the alginate hydrogel could also serve as a carrier of bioactive factors with capability to enhance cardiac function. For example, Ruvinov et al. injected the alginate hydrogel loaded with insulin like growth factor-1 (IGF-1) and hepatocyte growth factor (HGF) into the MI infarct area, and found that such hydrogel could sustainably release IGF-1 and HGF to effectively improve cardiac function by protecting myocardial cells and promoting angiogenesis, respectively [35].

In this work, we developed an injectable alginate-based composite hydrogel containing two bioactive factors with different functions aiming at the treatment of different stages of MI. In order to realize different release profiles of VEGF and BMP9, we chose silk fibroin (SF) microspheres as the carrier for loading BMP9. These microspheres were added to alginate impregnated with VEGF, followed by being crosslinked with calcium gluconate to form a composite hydrogel. We expected this composite hydrogel could rapidly release VEGF to facilitate angiogenesis in the early stage of MI and then sustainably release BMP9 to inhibit fibrosis formation in the long-term stage of MI, respectively. The *in vitro* release profiles were investigated, and *in vitro* and *in vivo* respective bioactivity of released VEGF and BMP9 were evaluated.

2. Experimental section

All the procedures related to animals were conducted with the approval of the Ethics Committee at Soochow University.

2.1. Preparation of SF microspheres loaded with BMP9

SF microspheres were prepared by a microfluidic device as indicated in Scheme S1 and the details were shown in Supporting Information. To prepare SF microspheres loaded with BMP9 (B/SF), BMP9 (R&D Systems, Bio-Techne, USA, 50 ng/μL, 8 μL) was dropped

Table 1
Abbreviations of samples used in this work.

Abbreviation	Description of sample
B/SF	SF microspheres loaded with BMP9
Gel	alginate crosslinked with Ca^{2+}
Gel + SF	Gel containing SF microspheres only
Gel + B	Gel containing BMP9 only
Gel + B/SF	Gel containing B/SF microspheres only
Gel + V	Gel containing VEGF only
Gel + B/SF + V	Gel containing both VEGF and B/SF microspheres

onto SF microspheres (0.4 mg), left for 12 h at 4 °C, and then freeze dried.

2.2. Preparation of the composite hydrogel

VEGF (Gibco, USA) and B/SF microspheres were added to alginate (Sigma-Aldrich, USA) solution, and then crosslinked with calcium gluconate (Sigma-Aldrich, USA) to prepare the composite hydrogel (Gel + B/SF + V). First, VEGF (50 ng/μL, 4 μL) was added to alginate aqueous solution (1.5% w/v, 100 μL), then 0.2 mg B/SF microspheres were added to the above solution, finally the solution was crosslinked with 100 μL calcium gluconate (Ca^{2+}). The hydrogels without any bioactive factors and with only VEGF or B/SF were prepared and used as controls. The abbreviations of the hydrogels used in this study were summarized in Table 1.

2.3. Characterization of the composite hydrogel

The morphologies of the SF microspheres and the composite hydrogel were observed by using scanning electron microscopy (SEM, S-4800; Hitachi, Tokyo, Japan). The diameter of the SF microspheres and the pore size of the hydrogel were calculated based on the SEM images.

The injectability of the hydrogel was evaluated by measuring the viscosity and the injectability via a 30G needle. The viscosity was measured by rheometer AR2000 (TA Instruments, USA) with the shear rate from 0.3 to 1 s^{-1} at 37 °C.

2.4. In vitro release behaviors of VEGF and BMP9 from the composite hydrogel

The *in vitro* release behaviors of VEGF and BMP9 from the composite hydrogel were evaluated by the enzyme linked immunosorbent assay (ELISA). In brief, 100 μL Gel + B/SF + V composite hydrogel and 200 μL phosphate buffer saline (PBS) were added to the upper chamber of a 24-well transwell plate, while 1 mL PBS was added to the lower chamber. At each time point (0, 1, 3, 5, 7, 10, 14, 21 and 28 day), 1 mL PBS was collected from the lower chamber and 1 mL fresh PBS was added. The collected PBS was stored at −80 °C for further analysis. The release amounts of VEGF and BMP9 at each time point were calculated by VEGF ELISA kit (Sigma-Aldrich, USA) and BMP9 ELISA kit (Sigma-Aldrich, USA), respectively. The cumulative release ratio was calculated as the ratio of the cumulative mass of VEGF or BMP9 released at each time interval to their initial input amount in the hydrogel, which was 100 ng for both BMP9 and VEGF.

2.5. Bioactivity of VEGF and BMP9 released from the composite hydrogel

The human umbilical vein endothelial cells (HUVECs, ScienCell Research Laboratories) tube formation assay was used to test the bioactivity of VEGF released from the hydrogel [36]. HUVECs were seeded on the culture plate coated by Matrigel at a density of 4×10^4 cells per well and cultured in endothelial cell growth medium-2 (EGM-2) containing VEGF released from the composited hydrogel for 5 h (named as VEGF (Gel)). HUVECs were cultured in EGM-2 without

VEGF (named as no VEGF) and in EGM-2 containing VEGF (10 ng/mL) that was directly added (named as VEGF) were used as negative and positive control, respectively. The formed tubes were observed using the optical microscopy (Olympus, IX51, Japan). The length and amount of formed tubes were quantified by using ImageJ software based on the bright-field images.

Primary cardiac fibroblasts were extracted from C57BL/6 mice (male, 8-week-old, average weight of 22–25 g) and passaged for 4 times. The cells were seeded in a 48-well plate at a density of 4.8×10^3 cells per well and cultured in 500 μL Dulbecco's modified Eagle medium (DMEM/F12) for 12 h, which was then replaced by 500 μL DMEM/F12 serum-free medium for 1 h. After that, the medium was replaced by 500 μL DMEM/F12 complete medium containing (i) 10 ng/mL TGF-β1 (named as TGF-β1), (ii) 10 ng/mL TGF-β1 and 10 ng/mL BMP9 (named as TGF-β1 + B), or (iii) 10 ng/mL TGF-β1 and BMP9 released from the composite hydrogel (named as TGF-β1 + B (Gel)). After 24 h of culture, the cells were stained with 4′,6-diamidino-2-phenylindole (DAPI) and immunofluorescent stained of α-smooth muscle actin (α-SMA) and observed using fluorescence microscopy (IX51 Olympus, Tokyo, Japan). The amount of α-SMA positive cells was quantified using ImageJ software.

2.6. Intramyocardial injection of the composite hydrogel to MI model

The mice MI model was established by permanently ligating the left anterior descending coronary artery (LAD) approximately 2 mm distal below the gap of left atrium appendage with 6–0 suture (Shanghai Pudong Jinhuan Medical Products Co. Ltd., China). The establishment of MI was considered successful following the visual appearance of pale discoloration and ST segment elevation in electrocardiogram. Mice in Sham group underwent an identical operation excepting without the ligation of the coronary artery. After the induction of MI, 10 μL of different hydrogels or PBS were administered via multiple injections into the border zone (4 points, each point 2.5 μL). A total of 90 mice were used and were randomly assigned into the following six groups ($n = 15$): Sham, PBS, Gel, Gel + B/SF, Gel + V and Gel + B/SF + V.

2.7. Histological analysis

Mice were anaesthetized after 28 days following MI or the hydrogel injection, and their hearts were excised and washed with PBS, fixed with 4% paraformaldehyde for 12 h. The samples were then dehydrated through an alcohol gradient (70%, 80%, 95% and 100%), and embedded in paraffin wax. 5-μm-thick tissue sections were prepared and stained with Masson's trichrome (Solarbio, China) to determine the infarct size. Immunohistochemical staining of CD31 (CST, USA) was also conducted to investigate neovascularization of infarcted tissue. The detailed procedures were shown in Supporting Information.

2.8. Western blot assay

Western blot assay was conducted to quantify specific protein levels in infarcted tissues. The samples were lysed by radio-immunoprecipitation assay buffer (RIPA buffer), and then centrifuged at 12,000 g at 4 °C for 10 min. The supernatant was collected, and the concentration of total protein in infarcted tissues was determined with bicinchoninic acid (BCA) assay (Absin, China). Protein were loaded and run on 10% sodium dodecyl sulphate-polyacrylamide gel electrophoresis (SDS-PAGE) gels and then transferred to polyvinylidene difluoride membranes. The membranes were then blocked with 5% skim milk for 1 h, incubated with Collagen type I (Col I) primary antibody (diluted with 3% bovine serum albumin) overnight at 4 °C and further incubated using the secondary antibody for another 1 h at room temperature. Glyceraldehyde 3-phosphate dehydrogenase (GAPDH) was used as an internal control. The labeled proteins were visualized by the enhanced chemiluminescence method and band intensity was normalized to the signal intensity of GAPDH using Image J software.

2.9. Echocardiographic analysis

Transthoracic echocardiography was performed to evaluate cardiac function at baseline, 7- and 28-day post-surgery using a Vevo 2100 system (VisualSonics, Canada). Under two-dimensional echocardiography, the long-axis images showing the left ventricular outflow tract and apex were obtained with a 40 MHz transducer. While the short-axis images were received after rotating it 90° clockwise. The M mode was collected and the left ventricular ejection fraction (LVEF) and the left ventricular fractional shortening (LVFS) were analyzed with its own system.

2.10. Statistical analysis

Experiments were performed in triplicate unless otherwise indicated. The data are expressed as the mean ± standard deviation. Statistical analysis was performed using OriginPro8.5 software. The p values were based on two-tailed Student's t-test. Differences of $*p < 0.05$, $**p < 0.01$ and $***p < 0.001$ were considered statistically significant.

3. Results and discussion

3.1. Characterization of the composite hydrogel

The composite hydrogel loaded with VEGF and BMP9 was prepared as illustrated in Scheme 1. First, SF microspheres were prepared using a coaxial needle system, and then loaded with BMP9 via physical adsorption. The resulted microspheres (B/SF) and VEGF were then added to alginate solution. Finally, calcium gluconate was added to the
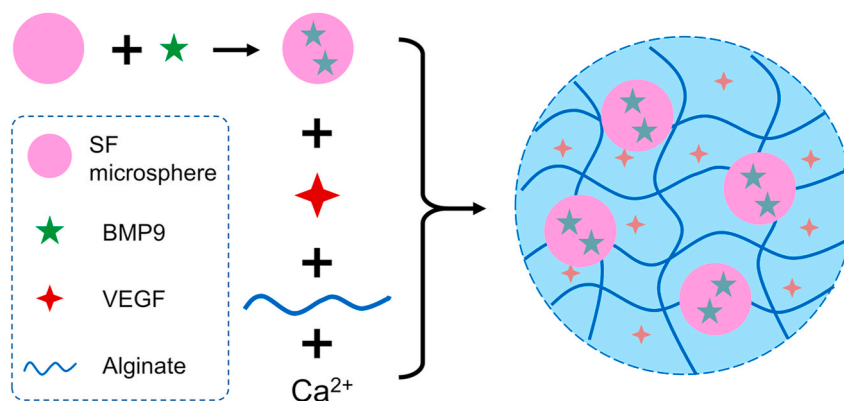
Scheme 1. Schematic of the preparation process of the composite hydrogel.
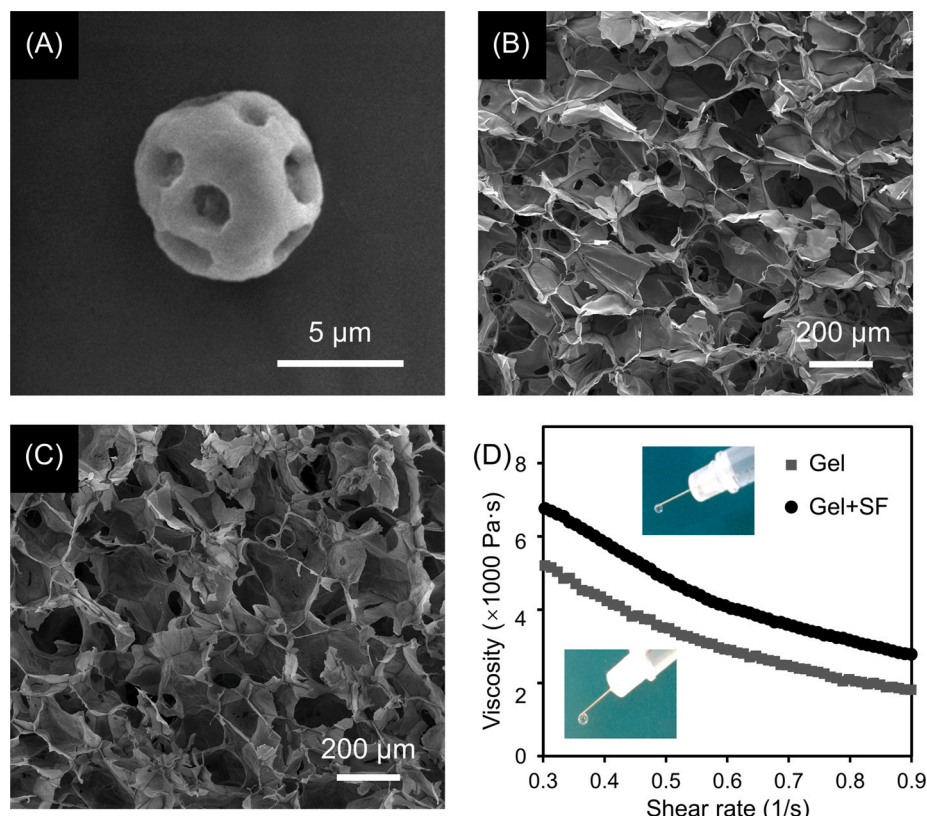
Fig. 1. Representative SEM images of (A) a SF microsphere, (B) Gel and (C) Gel + SF. (D) Change of viscosity of Gel and Gel + SF in response to shear rate. The insets showed that both of Gel and Gel + SF are injectable through a conventional syringe using a 30 G needle.

mixture to crosslink alginate, resulting in a composite hydrogel (Gel + B/SF + V). The hydrogels without any bioactive factors (Gel), and with only VEGF (Gel + V), BMP9 (Gel + B) or B/SF (Gel + B/SF) were prepared in a similar manner and used as controls.

The as-prepared SF microspheres showed a porous spherical structure with an average diameter of 7.2 ± 1.3 μm as observed by SEM (Fig. 1A). These microspheres were relatively stable after soaking in PBS at 37 °C for 28 days (Fig. S1, Supporting Information), in consistent with previous reports [37,38]. The pristine alginate hydrogel showed a porous network structure with an average pore size of 193.6 ± 31.8 μm (Fig. 1B), which decreased to 181.1 ± 21.6 μm after incorporation of SF microspheres that were evenly distributed in the composite hydrogel (Fig. 1C). Viscosity is an important property for injectable hydrogels. As shown in Fig. 1D, the viscosity of hydrogel increased after incorporation of SF microspheres. Both Gel and Gel + SF exhibited shear-thinning behavior (that is the viscosity decreases with an increase of shear rate) and were injectable through a conventional syringe.

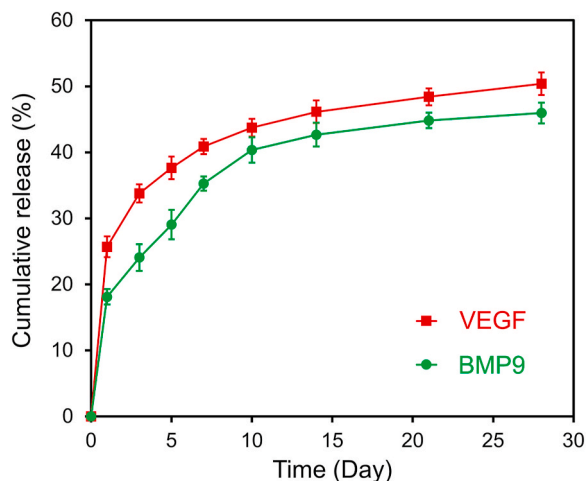### 3.2. In vitro release of VEGF and BMP9 from the composite hydrogel

The pathological process of MI is relatively complicated. In the early stage (within 7 days), it is mainly involved the irreversible necrosis of myocardial cells, the degradation of ECM, inflammatory response, etc., while fibrosis exists in the entire pathological process, lasting for more than 28 days [3,4]. According to the different stages of pathological process, different bioactive factors were used to treat MI [39,40]. Since fibrosis exists in the entire pathological process, the release of BMP9 needs to last relative longer compared with VEGF. The release profiles of two bioactive factors could be adjusted by selecting two biomaterials with different degradation rates [41], or by pre-loading one of the factors in a secondary carrier [42–44]. For example, we added SF microspheres encapsulated with bone morphogenetic protein-2 (BMP2)

into a SF scaffold, which was further functionalized with SDF-1 via physical adsorption. This composite scaffold showed rapid release of SDF-1 during the first few days, followed by a slow and sustained release of BMP2 for as long as three weeks, suggesting that the introduction of SF microspheres could successfully elongate the release time of one bioactive factor without influencing the release of another bioactive factor [42].

In the current study, the composite hydrogel with VEGF and SF microspheres encapsulated with BMP9 was designed to release VEGF rapidly in the early time to promote angiogenesis and improve the microenvironment; while the relatively sustained release of BMP9 in long-term can inhibit myocardial fibrosis, ultimately improving cardiac function after MI. The *in vitro* release profiles of VEGF and BMP9 from the composite hydrogel were investigated using the corresponding ELISA kits, and the results were shown in Fig. 2. The overall release of BMP9 from Gel + B/SF + V was comparatively slow compared with VEGF; the cumulative release of VEGF and BMP9 for 7 days was 40.9 ± 1.1% and 35.3 ± 1.1%, respectively. In addition, it is found that the release profile of BMP9 from Gel + B (in which BMP9 was directly loaded without using microspheres) was similar to that of VEGF from Gel + B/SF + V (Fig. S2, Supporting Information), indicating that the introduction of SF microspheres slowed down the release of BMP9 in the hydrogel to fulfill the sustained release purpose.

3.3. In vitro bioactivity of VEGF and BMP9 released from the composite hydrogel

Revascularization of ischemic myocardium is essential for myocardial tissue regeneration and functional recovery. It is demonstrated that VEGF can effectively promote the proliferation, migration and tube formation of endothelial cells, facilitating the formation of functional blood vessels in the infarcted area and improving the recovery of cardiac function after MI [15]. In this study, to investigate whether VEGF

Fig. 2. *In vitro* release profiles of VEGF (red curve) and BMP9 (green curve) from Gel + B/SF + V ($n = 3$). (For interpretation of the references to color in this figure legend, the reader is referred to the Web version of this article.)

released from the composite hydrogel retained the bioactivity, HUVEC-tube formation assay was performed. As shown in Fig. 3 and Fig. S3 (Supporting information), after culturing for 5 h, the length and amount of formed HUVEC tubes increased significantly in the medium containing VEGF (i.e. VEGF (Gel) group and VEGF group) compared to that in the cell culture medium without VEGF (no VEGF group). No statistical difference in tube length and tube amount between VEGF (Gel) group and VEGF group, indicating that VEGF released from the composite hydrogel retained its biological activity and was expected to promote angiogenesis in infarcted myocardium according to the previous report [31].

During the process of myocardial fibrosis, TGF-β1 is an important bioactive factor that induces the transformation of cardiac fibroblasts to myofibroblasts [45,46]. It is reported that the activity of TGF-β1 could

be inhibited by BMP9 and thus the cardiac function in HF was improved [19]. In this study, the effect of BMP9 released from the composite hydrogel on the conversion of primary cardiac fibroblasts to myofibroblasts was investigated by immunohistochemical staining assay. α-SMA immunohistochemical staining in cells were evaluated because α-SMA is a specific marker of myofibroblasts, and its expression level could be used to evaluate the transformation from cardiac fibroblasts to myofibroblasts [47,48]. As shown in Fig. 4, after 24 h of culture, α-SMA expression level in TGF-β1 group was obviously higher than that in no TGF-β1 group, indicating that TGF-β1 induced the transformation of cardiac fibroblasts to myofibroblasts. However, TGF-β1 + B and TGF-β1 + B (Gel) group expressed less α-SMA than TGF-β1 group, suggesting that the activity of TGF-β1 was inhibited by BMP9, and BMP9 released from hydrogel maintained the bioactivity. Taken together, these results demonstrated that the bioactive factors (VEGF and BMP9) released from the composite hydrogel still maintained their corresponding bioactivities.

3.4. In vivo angiogenesis study

After demonstration of the bioactivity of released VEGF and BMP9 from the composite hydrogel by *in vitro* assays, we further investigated the treatment of this hydrogel on MI model *in vivo*. For MI treatment, to lighten the heart load, the volume of intramyocardial injection fluid is often in the range of 10–20 μL and performed at multiple sites [49,50]. In this study, 10 μL of hydrogel was injected at 4 points (2.5 μL per point) in the infarct border zone.

Considering that the composite hydrogel could rapidly release VEGF *in vitro* and the released VEGF maintained its biological activity (Figs. 2 and 3), injection of this hydrogel into the peripheral area of infarction was expected to promote angiogenesis. CD31 is a specific marker of endothelial cells and can be used to monitor the neovascularization of infarct tissue [51]. In this study, to investigate neovascularization of infarcted tissues in mice, CD31 immunohistochemical staining was performed on the infarcted heart tissues 28 days after injection of Gel + B/SF + V; Gel, Gel + B/SF, Gel + V, and PBS were used as
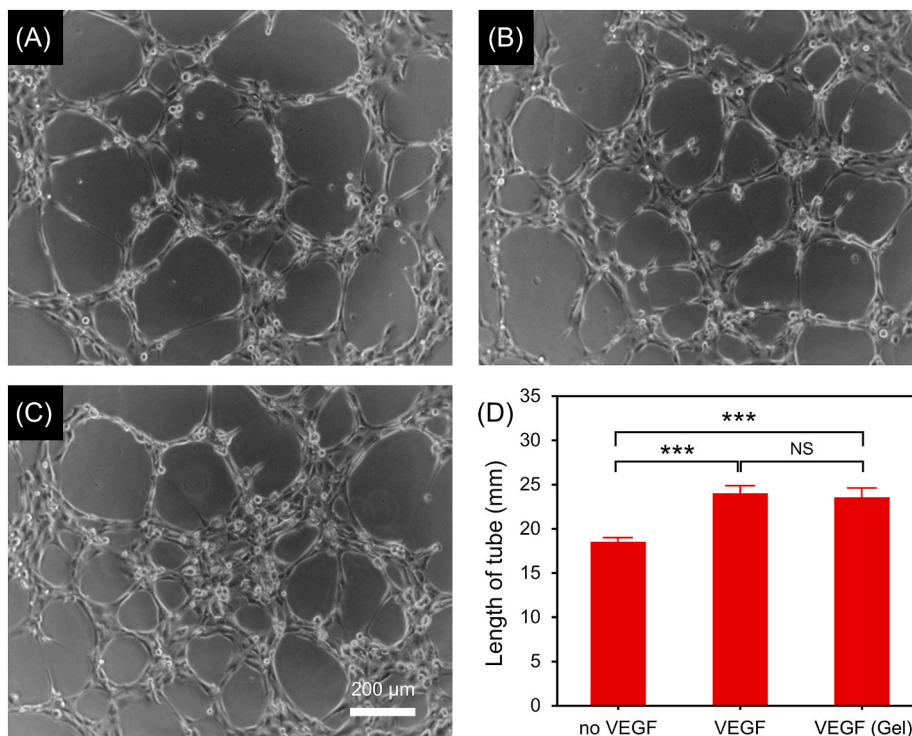

Fig. 3. (A–C) Representative microscopy images showing the formation of HUVEC tubes in the group of (A) no VEGF, (B) VEGF and (C) VEGF (Gel). The lengths of formed HUVEC tubes are shown in (D) ($n = 3$, ***$p < 0.001$).
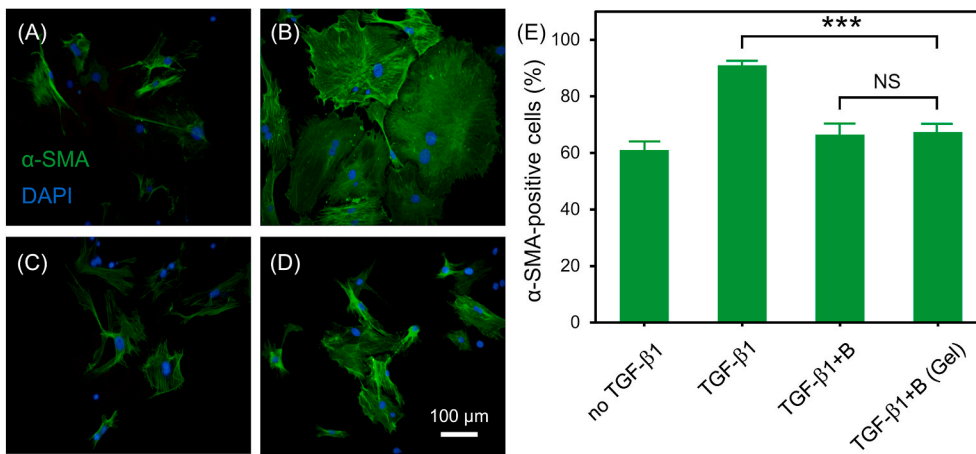
Fig. 4. (A–D) Representative fluorescence microscopy images of cardiac fibroblasts after 24 h of culture in different medium: (A) no TGF-β1, (B) TGF-β1, (C) TGF-β1 + B, (D) TGF-β1 + B (Gel). (blue: DAPI; green: α-SMA). (E) The statistical results of the ratio of α-SMA positive cells to all cells ($n = 3$, ***$p < 0.001$). (For interpretation of the references to color in this figure legend, the reader is referred to the Web version of this article.)
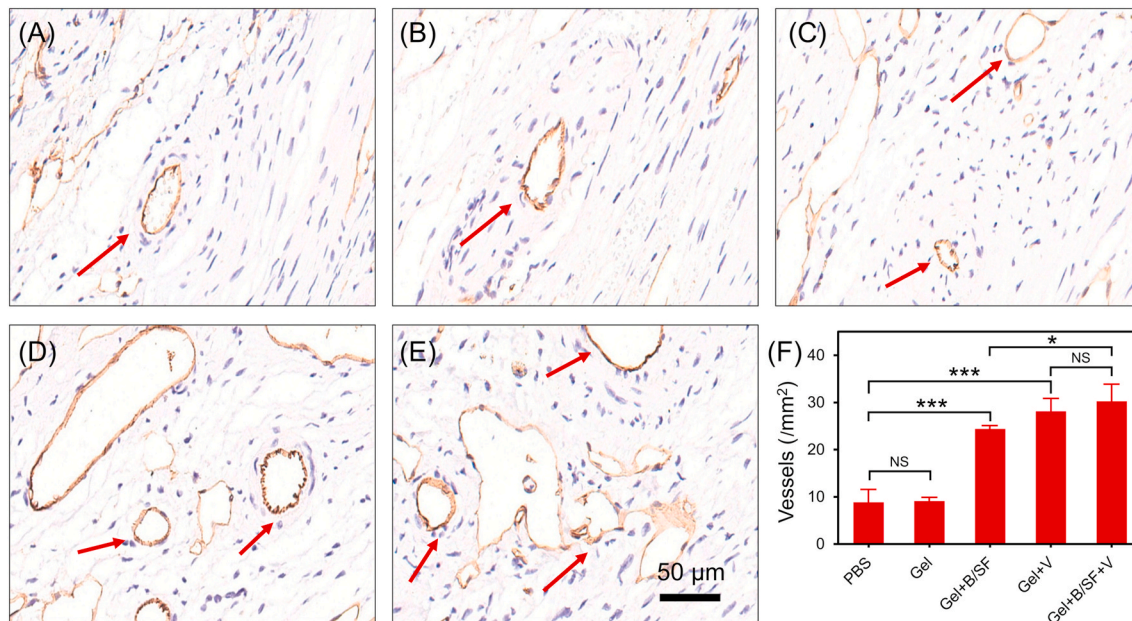
Fig. 5. (A–E) Representative images of infarcted sections performed by immunohistochemical staining of CD31 (red arrows refer to newly formed blood vessels in the infarcted area). (A) PBS, (B) Gel, (C) Gel + B/SF, (D) Gel + V, (E) Gel + B/SF + V. (F) Quantified number of vessels in the infarct area ($n = 6$, *$p < 0.05$, ***$p < 0.001$). (For interpretation of the references to color in this figure legend, the reader is referred to the Web version of this article.)
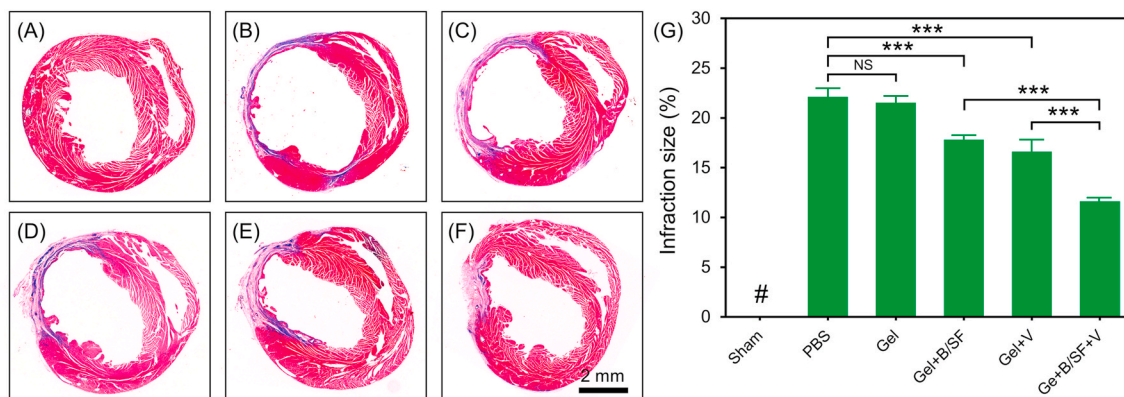
Fig. 6. Assessment of fibrosis in the infarct area 28 days post-MI. (A–F) Representative images of infarcted sections performed by Masson's trichrome staining. (A) Sham, (B) PBS, (C) Gel, (D) Gel + B/SF, (E) Gel + V, (F) Gel + B/SF + V. (G) Quantitative analysis of the infarction size as expressed by the ratio of infarct area to total left ventricular area ($n = 6$, ***$p < 0.001$). # means no detectable infract area.
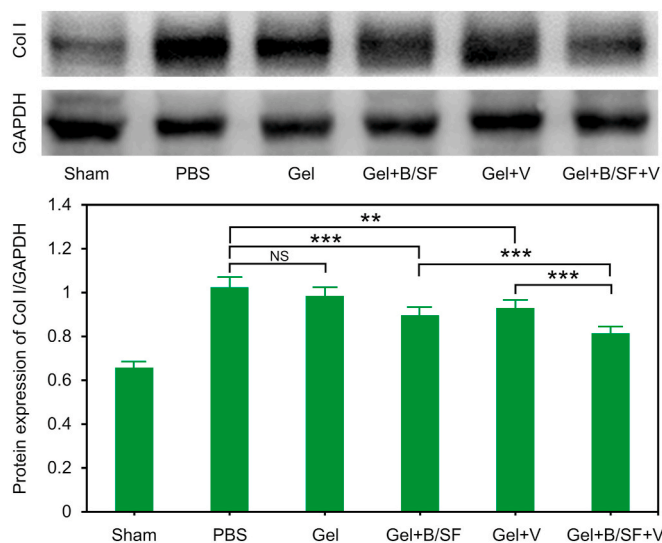
Fig. 7. Representative ratios of Col I to GAPDH based on the results of western blot analysis from three independent experiments (**$p < 0.01$, ***$p < 0.001$).

controls (Fig. 5A–E). Compared with PBS group, there was no significant change in the number of newly formed vessels in Gel group. In contrast, more newly formed vessels were observed for all the groups with hydrogels containing bioactive factors (Fig. 5F). In particular, the groups of hydrogels containing VEGF (Gel + V and Gel + B/SF + V) showed the highest number of vessels, suggesting the promotion effect of VEGF on angiogenesis [31]. The released VEGF would contribute to the blood recovery of infarcted tissue by providing nutrients and oxygen to cells in the peripheral area of the infarcted area, improving the microenvironment of the infarcted area and heart function [39]. In addition, it is suggested that BMP9 also exhibited a certain pro-angiogenic function, similar to the previous report [19].

3.5. In vivo fibrosis study

Fibrosis can lead to cardiac remodeling and dysfunction [52]. To improve cardiac function after MI, different methods have been developed to inhibit myocardial fibrosis. For example, daily intraperitoneal injection of Fasudil to inhibit the TGF-β1-TAK1 pathway could effectively reduce myocardial fibrosis and improve cardiac function after MI [53]. In addition, injection of an angiotensin receptor neprilysin inhibitors (ARNi) can inhibit AngII, and then reduce collagen accumulation, thus inhibiting myocardial fibrosis [54]. Recently, Morine et al. reported a new role for BMP9 as an endogenous inhibitor of cardiac fibrosis. On the one hand, BMP9 could attenuate the phosphorylation of Smad3, the downstream effector of TGF-β1, thereby weakening the synthesis of type I collagen induced by TGF-β1. On the other hand, BMP9 could promote activin receptor-like kinase 1 (ALK-1)-mediated phosphorylation of Smad1 and neutralize endoglin activity to limit cardiac fibrosis [19]. In this work, we also founded that the released BMP9 from the composite hydrogel showed capability to inhibit transformation from cardiac fibroblasts to myofibroblasts *in vitro* (Fig. 4). Therefore, the composite hydrogel was injected into the infarct border zone of mice heart to verify its effects on myocardial fibrosis *in vivo*. After 28 days of injection, the pathological sections of the heart were taken for Masson's trichromestaining and the infarction size was calculated (Fig. 6). The infarction size was 22.1 ± 0.9% and 21.5 ± 0.7% for PBS group and Gel group, respectively. Compared with these two groups, the hydrogel contained bioactive factors showed significantly decreased infarction size, which was 17.8 ± 0.4%, 16.6 ± 1.3% and 11.6 ± 0.4% for Gel + B/SF group, Gel + V group and Gel + B/SF + V group, respectively. Among these hydrogels, Gel + B/SF + V showed the best anti-fibrosis effect to inhibit the further expansion of infarct area.

Collagen I (Col I) is an essential component of cardiac ECM. However, large accumulation of Col I leads to increased myocardial fibrosis in MI [55]. To further test the influence of the composite hydrogel on myocardial fibrosis, the secretion level of Col I in MI tissue was analyzed by Western Blot assay after 28 days of hydrogel injection. As shown in Fig. 7, there was no significant difference in secretion of Col I between Gel and PBS group. Compared with PBS group, Gel + B/SF, Gel + V and Gel + B/SF + V groups showed less amount of Col I, and Gel + B/SF + V group showed the least amount of Col I, consistent with the results of Masson staining. Taken together, the combination of VEGF and BMP9 in the hydrogel showed a kind of collaborative effect on inhibiting fibrosis than the hydrogel contains only VEGF or BMP9.

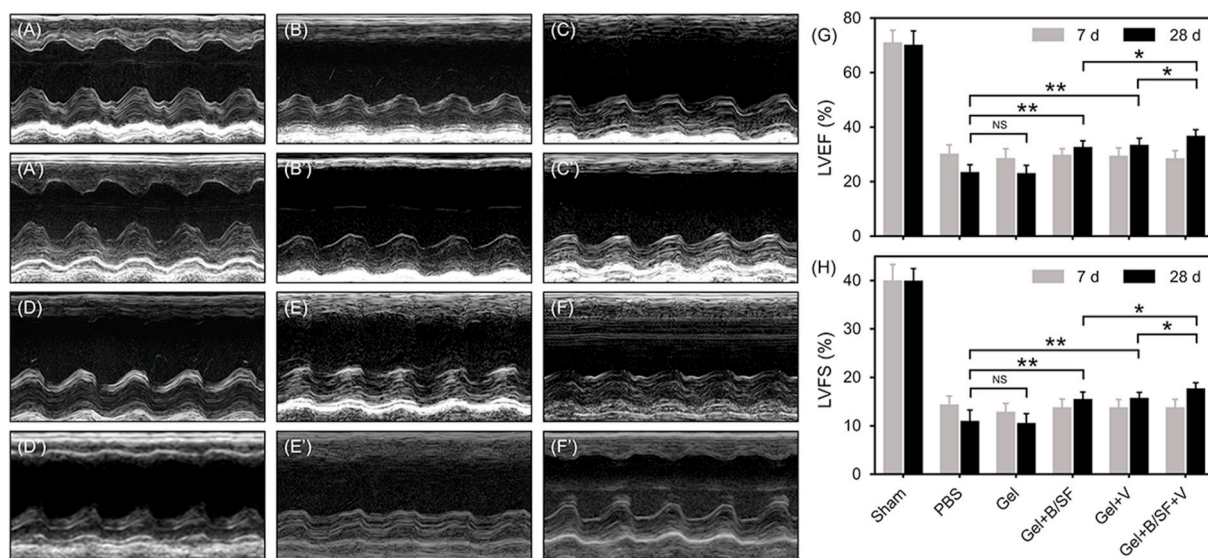**Fig. 8.** Echocardiography of MI in mice administered with different hydrogels or PBS by intramyocardial injection. Representative M-mode images at 7th day (A–F) and 28th day (A′-F′) post-MI. (A, A′) Sham, (B, B′) PBS, (C, C′) Gel, (D, D′) Gel + B/SF, (E, E′) Gel + V, (F, F′) Gel + B/SF + V. Quantitative analysis of the LVEF (G) and LVFS (H) at the indicated time points ($n = 15$, *$p < 0.05$,**$p < 0.01$).

3.6. In vivo evaluation of heart function

The cardiac function of the mice was evaluated by echocardiography after 7 and 28 days of injection. At 28th day, the results indicated that the contraction of the anterior left ventricular wall in the groups that contained VEGF or/and BMP9 (Gel + B/SF, Gel + V and Gel + B/SF + V) was significantly increased compared with that of PBS group or Gel group; the heart contraction is most obvious in Gel + B/SF + V group compared with the other groups (Fig. 8A'-8F'). LVEF and LVFS values of each group were also analyzed. For Sham group, the LVEF and LVFS were 71.1 ± 7.4% and 40.0 ± 6.3%, respectively at 7th day after MI, which were quite close to the heart function of normal mice as reported by other groups [56,57]. At 28th day after surgery, the hydrogel contained VEGF or/and BMP9 were significantly increase compared with PBS group or Gel group; the LVEF showed the highest in Gel + B/SF + V compared with the other hydrogels. Compared with that at 7th day, the LVEF at 28th day was increased by 2.9%, 4.0% and 8.3% for Gel + B/SF, Gel + V and Gel + B/SF + V groups, respectively, while decreased by 6.6% for PBS group and 5.5% for Gel group (Fig. 8G). LVFS showed the similar trend with that of LVEF (Fig. 8H).

Based on the above results, the injection of alginate hydrogel without bioactive factors showed no obvious effects on the recovery of cardiac function, similar to the results as previously reported [58]. While the injection of Gel impregnant with VEGF or/and BMP9 could improve the cardiac function, and among these hydrogels, the composite hydrogel Gel + B/SF + V showed the best performance. That is, compared with single-factor system (Gel + B/SF or Gel + V), the dual-factor composite hydrogel Gel + B/SF + V had lower degree of fibrosis, smaller infarct size and better cardiac function, indicating that the combination of VEGF and BMP9 in alginate hydrogel could promote angiogenesis and inhibit fibrosis after MI.

4. Conclusion

In summary, we developed an injectable alginate-based composite hydrogel incorporated with VEGF and SF microspheres encapsulated with BMP9 to realize dual-release of VEGF and BMP9. Such system could release VEGF rapidly to promote angiogenesis, and release BMP9 sustainably to inhibit fibrosis, meeting the bioactivity requirement and timeline of each MI stage to enhance heart function. After injection in MI heart, such combination therapy could effectively accelerate the vessel formation and inhibit the fibrosis formation in a MI mouse model to improve cardiac functions. The application of this composite hydrogel may provide a powerful platform in the treatment of MI for clinical application.

CRediT authorship contribution statement

Yong Wu: Conceptualization, Investigation, Methodology, Writing - original draft. **Tianqi Chang:** Validation, Methodology. **Weiqian Chen:** Investigation, Software. **Xiaoyu Wang:** Methodology. **Jingjing Li:** Investigation. **Yueqiu Chen:** Visualization. **You Yu:** Software. **Zhenya Shen:** Funding acquisition, Supervision. **Qian Yu:** Conceptualization, Writing - review & editing. **Yanxia Zhang:** Conceptualization, Supervision, Writing - review & editing, Project administration.

Declaration of competing interest

The authors declare no conflicts of interest.

Acknowledgments

Appendix A. Supplementary data

Supplementary data to this article can be found online at https://doi.org/10.1016/j.bioactmat.2020.08.031.

References

[1] S.S. Virani, A. Alonso, E.J. Benjamin, M.S. Bittencourt, C.W. Callaway, A.P. Carson, A.M. Chamberlain, A.R. Chang, S. Cheng, F.N. Delling, L. Djousse, M.S.V. Elkind, J.F. Ferguson, M. Fornage, S.S. Khan, B.M. Kissela, K.L. Knutson, T.W. Kwan, D.T. Lackland, T.T. Lewis, J.H. Lichtman, C.T. Longenecker, M.S. Loop, P.L. Lutsey, S.S. Martin, K. Matsushita, A.E. Moran, M.E. Mussolino, A.M. Perak, W.D. Rosamond, G.A. Roth, U.K.A. Sampson, G.M. Satou, E.B. Schroeder, S.H. Shah, C.M. Shay, N.L. Spartano, A. Stokes, D.L. Tirschwell, L.B. VanWagner, C.W. Tsao, Heart disease and stroke statistics-2020 update: a report from the American Heart Association, Circulation 141 (2020) e139–e596.

[2] D.K. Arnett, R.S. Blumenthal, M.A. Albert, A.B. Buroker, Z.D. Goldberger, E.J. Hahn, C.D. Himmelfarb, A. Khera, D. Lloyd-Jones, J.W. McEvoy, E.D. Michos, M.D. Miedema, D. Munoz, S.C. Smith, S.S. Virani, K.A. Williams, J. Yeboah, B. Ziaeian, ACC/AHA guideline on the primary prevention of cardiovascular disease: a report of the American College of Cardiology/American Heart Association task force on clinical practice guidelines, Circulation 140 (2019) (2019) e596–e646.

[3] E. Ruvinov, S. Cohen, Alginate biomaterial for the treatment of myocardial infarction: progress, translational strategies, and clinical outlook from ocean algae to patient bedside, Adv. Drug Deliv. Rev. 96 (2016) 54–76.

[4] S.D. Prabhu, N.G. Frangogiannis, The biological basis for cardiac repair after myocardial infarction from inflammation to fibrosis, Circ. Res. 119 (2016) 91–112.

[5] P.W. Serruys, M. Morice, A.P. Kappetein, A. Colombo, D.R. Holmes, M.J. Mack, E. Ståhle, T.E. Feldman, M. Brand, E.J. Bass, N.V. Dyck, K. Leadley, K.D. Dawkins, F.W. Mohr, Percutaneous coronary intervention versus coronary-artery bypass grafting for severe coronary artery disease, N, Engl. J. Med. 360 (2009) 961–972.

[6] G.W. Stone, A.P. Kappetein, J.F. Sabik, S.J. Pocock, M.C. Morice, J. Puskas, D.E. Kandzari, D. Karmpaliotis, W.M. Brown 3rd, N.J. Lembo, A. Banning, B. Merkely, F. Horkay, P.W. Boonstra, A.J. van Boven, I. Ungi, G. Bogats, S. Mansour, N. Noiseux, M. Sabate, J. Pomar, M. Hickey, A. Gershlick, P.E. Buszman, A. Bochenek, E. Schampaert, P. Page, R. Modolo, J. Gregson, C.A. Simonton, R. Mehran, I. Kosmidou, P. Genereux, A. Crowley, O. Dressler, P.W. Serruys, Five-year outcomes after PCI or CABG for left main coronary disease, N. Engl. J. Med. 381 (2019) 1820–1830.

[7] W. Jiang, D. Rutherford, T. Vuong, H. Liu, Nanomaterials for treating cardiovascular diseases: a review, Bioact. Mater. 2 (2017) 185–198.

[8] Y. Jiang, X.L. Lian, Heart regeneration with human pluripotent stem cells: prospects and challenges, Bioact. Mater. 5 (2020) 74–81.

[9] E.T. Roche, C.L. Hastings, S.A. Lewin, D.E. Shvartsman, Y. Brudno, N.V. Vasilyev, F.J. O'Brien, C.J. Walsh, G.P. Duffy, D.J. Mooney, Comparison of biomaterial delivery vehicles for improving acute retention of stem cells in the infarcted heart, Biomaterials 35 (2014) 6850–6858.

[10] P.V. Johnston, C.W. Hwang, V. Bogdan, K.J. Mills, E.R. Eggan, A. Leszczynska, K.C. Wu, D.A. Herzka, J.A. Brinker, S.P. Schulman, M. Banerjee, V. Florea, M. Natsumeda, B. Tompkins, W. Balkan, J.M. Hare, G.F. Tomaselli, R.G. Weiss, G. Gerstenblith, Intravascular stem cell bioreactor for prevention of adverse remodeling after myocardial infarction, J. Am. Heart Assoc. 8 (2019) e012351.

[11] J.M. Tang, J.N. Wang, L. Zhang, F. Zheng, J.Y. Yang, X. Kong, L.Y. Guo, L. Chen, Y.Z. Huang, Y. Wan, S.Y. Chen, VEGF/SDF-1 promotes cardiac stem cell mobilization and myocardial repair in the infarcted heart, Cardiovasc. Res. 91 (2011) 402–411.

[12] S. Windmolders, A. De Boeck, R. Koninckx, A. Daniels, O. De Wever, M. Bracke, M. Hendrikx, K. Hensen, J.-L. Rummens, Mesenchymal stem cell secreted platelet derived growth factor exerts a pro-migratory effect on resident cardiac atrial appendage stem cells, J. Mol. Cell. Cardiol. 66 (2014) 177–188.

[13] K. Huang, S. Hu, K. Cheng, A new era of cardiac cell therapy: opportunities and challenges, Adv. Healthcare Mater. 8 (2019) 1801011.

[14] H.K. Awada, N.R. Johnson, Y. Wang, Sequential delivery of angiogenic growth factors improves revascularization and heart function after myocardial infarction, J. Contr. Release 207 (2015) 7–17.

[15] X. Hao, E.A. Silva, A. Mansson-Broberg, K.-H. Grinnemo, A.J. Siddiqui, G. Dellgren, E. Wardell, L.A. Brodin, D.J. Mooney, C. Sylven, Angiogenic effects of sequential release of VEGF-A(165) and PDGF-BB with alginate hydrogels after myocardial infarction, Cardiovasc. Res. 75 (2007) 178–185.

[16] J.G. Travers, F.A. Kamal, J. Robbins, K.E. Yutzey, B.C. Blaxall, Cardiac fibrosis the fibroblast awakens, Circ. Res. 118 (2016) 1021–1040.

[17] J.J. Santiago, A.L. Dangerfield, S.G. Rattan, K.L. Bathe, R.H. Cunnington, J.E. Raizman, K.M. Bedosky, D.H. Freed, E. Kardami, I.M.C. Dixon, Cardiac fibroblast to myofibroblast differentiation in vivo and in vitro: expression of focal

adhesion components in neonatal and adult rat ventricular myofibroblasts, Dev. Dynam. 239 (2010) 1573–1584.

[18] X. Li, H. Zhao, C. Qi, Y. Zeng, F. Xu, Y. Du, Direct intercellular communications dominate the interaction between adipose-derived MSCs and myofibroblasts against cardiac fibrosis, Protein Cell 6 (2015) 735–745.

[19] K.J. Morine, X. Qiao, S. York, P.S. Natov, V. Paruchuri, Y. Zhang, M.J. Aronovitz, R.H. Karas, N.K. Kapur, Bone morphogenetic protein 9 reduces cardiac fibrosis and improves cardiac function in heart failure, Circulation 138 (2018) 513–526.

[20] A. Le Bras, Heart failure: BMP9 is an inhibitor of cardiac fibrosis, Nat. Rev. Cardiol. 15 (2018) 254-254.

[21] A. Pal, B.L. Vernon, M. Nikkhah, Therapeutic neovascularization promoted by injectable hydrogels, Bioact. Mater. 3 (2018) 389–400.

[22] G. Liu, L. Li, D. Huo, Y. Li, Y. Wu, L. Zeng, P. Cheng, M. Xing, W. Zeng, C. Zhu, A VEGF delivery system targeting MI improves angiogenesis and cardiac function based on the tropism of MSCs and layer-by-layer self-assembly, Biomaterials 127 (2017) 117–131.

[23] T. Su, K. Huang, M.A. Daniele, M.T. Hensley, A.T. Young, J. Tang, T.A. Allen, A.C. Vandergriff, P.D. Erb, F.S. Ligler, K. Cheng, Cardiac stem cell patch integrated with microengineered blood vessels promotes cardiomyocyte proliferation and neovascularization after acute myocardial infarction, ACS Appl. Mater. Interfaces 10 (2018) 33088–33096.

[24] E. Mihalko, K. Huang, E. Sproul, K. Cheng, A.C. Brown, Targeted treatment of lschemic and fibrotic complications of myocardial infarction using a dual-delivery microgel therapeutic, ACS Nano 12 (2018) 7826–7837.

[25] A. Hasan, A. Khattab, M.A. Islam, K. Abou Hweij, J. Zeitouny, R. Waters, M. Sayegh, M.M. Hossain, A. Paul, Injectable hydrogels for cardiac tissue repair after myocardial infarction, Adv. Sci. 2 (2015) 1500122.

[26] J. Chen, X. Zou, Self-assemble peptide biomaterials and their biomedical applications, Bioact. Mater. 4 (2019) 120–131.

[27] C. Liu, X. Xu, J. Zhou, J. Yan, D. Wang, H. Zhang, Redox-responsive tumor targeted dual-drug loaded biocompatible metal-organic frameworks nanoparticles for enhancing anticancer effects, BMC Mater 2 (2020), https://doi.org/10.1186/s42833-020-00013-y.

[28] W. Chen, X. Tian, W. He, J. Li, Y. Feng, G. Pan, Emerging functional materials based on chemically designed molecular recognition, BMC Mater 2 (2020), https://doi.org/10.1186/s42833-019-0007-1.

[29] Q.Q. Wang, Y. Liu, C.-J. Zhang, C. Zhang, P. Zhu, Alginate/gelatin blended hydrogel fibers cross-linked by Ca^{2+} and oxidized starch: preparation and properties, Mater. Sci. Eng. C 99 (2019) 1469–1476.

[30] B. Pena, M. Laughter, S. Jett, T.J. Rowland, M.R.G. Taylor, L. Mestroni, D. Park, Injectable hydrogels for cardiac tissue engineering, Macromol. Biosci. 18 (2018) 1800079.

[31] J. Rodness, A. Mihic, Y. Miyagi, J. Wu, R.D. Weisel, R.-K. Li, VEGF-loaded microsphere patch for local protein delivery to the ischemic heart, Acta Biomater. 45 (2016) 169–181.

[32] J. Feng, Y. Wu, W. Chen, J. Li, X. Wang, Y. Chen, Y. Yu, Z. Shen, Y. Zhang, Sustained release of bioactive IGF-1 from a silk fibroin microsphere-based injectable alginate hydrogel for the treatment of myocardial infarction, J. Mater. Chem. B 8 (2020) 308–315.

[33] T. Hao, J. Li, F. Yao, D. Dong, Y. Wang, B. Yang, C. Wang, Injectable fullerenol/alginate hydrogel for suppression of oxidative stress damage in brown adipose-derived stem cells and cardiac repair, ACS Nano 11 (2017) 5474–5488.

[34] J. Leor, S. Tuvia, V. Guetta, F. Manczur, D. Castel, U. Willenz, O. Petnehazy, N. Landa, M.S. Feinberg, E. Konen, O. Goitein, O. Tsur-Gang, M. Shaul, L. Klapper, S. Cohen, Intracoronary injection of in situ forming alginate hydrogel reverses left ventricular remodeling after myocardial infarction in swine, J. Am. Coll. Cardiol. 54 (2009) 1014–1023.

[35] E. Ruvinov, J. Leor, S. Cohen, The promotion of myocardial repair by the sequential delivery of IGF-1 and HGF from an injectable alginate biomaterial in a model of acute myocardial infarction, Biomaterials 32 (2011) 565–578.

[36] C. Sun, S.B. Feng, Z.W. Cao, J.J. Bei, Q. Chen, X.J. Xu, Z. Zhou, Z.P. Yu, H.Y. Hu, Up-regulated expression of matrix metalloproteinases in endothelial cells mediates platelet microvesicle-induced angiogenesis, Cell. Physiol. Biochem. 41 (2017) 2319–2332.

[37] G.B. Chen, R.N. Wei, X. Huang, F.P. Wang, Z.M. Chen, Synthesis and assessment of sodium alginate-modified silk fibroin microspheres as potential hepatic arterial embolization agent, Int. J. Biol. Macromol. 155 (2020) 1450–1459.

[38] L.B. Shi, H.X. Cai, L.K. Chen, Y. Wu, S.A. Zhu, X.N. Gong, Y.X. Xia, H.W. Ouyang, X.H. Zou, Tissue engineered bulking agent with adipose-derived stem cells and silk fibroin microspheres for the treatment of intrinsic urethral sphincter deficiency, Biomaterials 35 (2014) 1519–1530.

[39] H.K. Awada, D.W. Long, Z. Wang, M.P. Hwang, K. Kim, Y. Wang, A single injection of protein-loaded coacervate-gel significantly improves cardiac function post infarction, Biomaterials 125 (2017) 65–80.

[40] H.K. Awada, L.A. Johnson, T.K. Hitchens, L.M. Foley, Y. Wang, Factorial design of experiments to optimize multiple protein delivery for cardiac repair, ACS Biomater. Sci. Eng. 2 (2016) 879–886.

[41] A. Cittadini, M.G. Monti, V. Petrillo, G. Esposito, G. Imparato, A. Luciani, F. Urciuolo, E. Bobbio, C.F. Natale, L. Sacca, P.A. Netti, Complementary therapeutic effects of dual delivery of insulin-like growth factor-1 and vascular endothelial growth factor by gelatin microspheres in experimental heart failure, Eur. J. Heart Fail. 13 (2011) 1264–1274.

[42] X. Shen, Y. Zhang, Y. Gu, Y. Xu, Y. Liu, B. Li, L. Chen, Sequential and sustained release of SDF-1 and BMP-2 from silk fibroin-nanohydroxyapatite scaffold for the enhancement of bone regeneration, Biomaterials 106 (2016) 205–216.

[43] D.M. Nelson, R. Hashizume, T. Yoshizumi, A.K. Blakney, Z. Ma, W.R. Wagner, Intramyocardial injection of a synthetic hydrogel with delivery of bFGF and IGF1 in a rat model of ischemic cardiomyopathy, Biomacromolecules 15 (2014) 1–11.

[44] W. Zhang, C. Ling, A. Zhang, H. Liu, Y. Jiang, X. Li, R. Sheng, Q. Yao, J. Chen, An all-silk-derived functional nanosphere matrix for sequential biomolecule delivery and in situ osteochondral regeneration, Bioact. Mater. 5 (2020) 832–843.

[45] H. Khalil, O. Kanisicak, V. Prasad, R.N. Correll, X. Fu, T. Schips, R.J. Vagnozzi, R. Liu, H. Thanh, S.-J. Lee, J. Karch, J.D. Molkentin, Fibroblast-specific TGF-beta-Smad2/3 signaling underlies cardiac fibrosis, J. Clin. Invest. 127 (2017) 3770–3783.

[46] S. Rosenkranz, TGF-beta(1) and angiotensin networking in cardiac remodeling, Cardiovasc. Res. 63 (2004) 423–432.

[47] K. Hao, W. Lei, H. Wu, J. Wu, Z. Yang, S. Yan, X.-A. Lu, J. Li, X. Xia, X. Han, W. Deng, G. Zhong, Z.A. Zhao, S. Hu, LncRNA-Safe contributes to cardiac fibrosis through Safe-Sfrp2-HuR complex in mouse myocardial infarction, Theranostics 9 (2019) 7282–7297.

[48] H.Y. Song, M.Y. Kim, K.H. Kim, I.H. Lee, S.H. Shin, J.S. Lee, J.H. Kim, Synovial fluid of patients with rheumatoid arthritis induces alpha-smooth muscle actin in human adipose tissue-derived mesenchymal stem cells through a TGF-beta 1-dependent mechanism, Exp. Mol. Med. 42 (2010) 565–573.

[49] S.T. Wall, J.C. Walker, K.E. Healy, M.B. Ratcliffe, J.M. Guccione, Theoretical impact of the injection of material into the myocardium: a finite element model simulation, Circulation 114 (2006) 2627–2635.

[50] Z.A. Zhao, X. Han, W. Lei, J. Li, Z. Yang, J. Wu, M. Yao, X.A. Lu, L. He, Y. Chen, B. Zhou, S. Hu, Lack of cardiac improvement after cardiosphere-derived cell transplantation in aging mouse hearts, Circ. Res. 123 (2018) e21–e31.

[51] H. Kim, H.J. Cho, S.W. Kim, B.L. Liu, Y.J. Choi, J. Lee, Y.D. Sohn, M.Y. Lee, M.A. Houge, Y.S. Yoon, CD31(+) cells represent highly angiogenic and vasculogenic cells in bone marrow novel role of nonendothelial CD31(+) cells in neovascularization and their therapeutic effects on ischemic vascular disease, Circ. Res. 107 (2010) 602–614.

[52] R.G. Gourdie, S. Dimmeler, P. Kohl, Novel therapeutic strategies targeting fibroblasts and fibrosis in heart disease, Nat. Rev. Drug Discov. 15 (2016) 620–638.

[53] Q. Li, Y. Xu, X. Li, Y. Guo, G. Liu, Inhibition of Rho-kinase ameliorates myocardial remodeling and fibrosis in pressure overload and myocardial infarction: role of TGF-beta1-TAK1, Toxicol. Lett. 211 (2012) 91–97.

[54] T.G. von Lueder, B.H. Wang, A.R. Kompa, L. Huang, R. Webb, P. Jordaan, D. Atar, H. Krum, Angiotensin receptor neprilysin inhibitor LCZ696 attenuates cardiac remodeling and dysfunction after myocardial infarction by reducing cardiac fibrosis and hypertrophy, Circ, Heart Fail. 8 (2015) 71–78.

[55] S. Hinderer, K. Schenke-Layland, Cardiac fibrosis - a short review of causes and therapeutic strategies, Adv. Drug Deliv. Rev. 146 (2019) 77–82.

[56] H. Mu, H. Liu, J. Zhang, J. Huang, C. Zhu, Y. Lu, Y. Shi, Y. Wang, Ursolic acid prevents doxorubicin-induced cardiac toxicity in mice through eNOS activation and inhibition of eNOS uncoupling, J. Cell Mol. Med. 23 (2019) 2174–2183.

[57] E. Gao, Y.H. Lei, X. Shang, Z.M. Huang, L. Zuo, M. Boucher, Q. Fan, J.K. Chuprun, X.L. Ma, W.J. Koch, A novel and efficient model of coronary artery ligation and myocardial infarction in the mouse, Circ. Res. 107 (2010) 1445–1453.

[58] K. Lv, Q. Li, L. Zhang, Y. Wang, Z. Zhong, J. Zhao, X. Lin, J. Wang, K. Zhu, C. Xiao, C. Ke, S. Zhong, X. Wu, J. Chen, H. Yu, W. Zhu, X. Li, B. Wang, R. Tang, J.A. Wang, J. Huang, X. Hu, Incorporation of small extracellular vesicles in sodium alginate hydrogel as a novel therapeutic strategy for myocardial infarction, Theranostics 9 (2019) 7403–7416.